

RESEARCH ARTICLE

Short Term Wind Speed Prediction Based on VMD and DBN Combined Model Optimized by Improved Sparrow Intelligent Algorithm

LIJUAN ZHU AND WEI HU

School of Information Engineering, Xinjiang Institute of Technology, Aksu 843015, China
School of Electrical Engineering, Xinjiang University, Urumqi 830047, China

Corresponding author: Wei Hu (434870858@qq.com)


This work was supported by the Natural Science Foundation of Xinjiang Uygur Autonomous Region under Grant 2022D01C355.

ABSTRACT Accurate wind speed prediction can help the power department to perceive the change rule of wind power in advance, reduce the impact of wind power grid connection, and then improve the wind power consumption rate. Therefore, an optimized variational modal decomposition (OVMD) method combined with optimized deep belief neural network (ODBN) is proposed to predict wind speed. First, the original wind speed data are processed by OVMD method, then the decomposed data are predicted by ODBN method, and the predicted component values are superimposed to obtain the wind speed prediction results. Taking the actual wind speed data of a certain area in Northwest China as an example, the proposed combined model is compared with common prediction methods such as DBN, long short term memory (LSTM), extreme learning machine (ELM), BP neural network, etc. The experimental results show that its RMSE decreases by 0.4494, 0.4778, 0.6217 and 0.6587, and its MAPE decreases by 10.3554%, 11.5484%, 14.6226% and 15.9493% respectively. The results verify the effectiveness of the prediction model.

INDEX TERMS Wind farm, wind speed, prediction accuracy, VMD, DBN.

NOMENCLATURE

VMD	Variational modal decomposition.	CEEMDAN	Complete ensemble empirical mode decomposition with adaptive noise.
ODBN	Optimized deep belief neural network.	ST	Safe threshold.
DBN	Deep belief network.	PIP	Proportion of investigator population.
OVMD	Optimized variational modal decomposition.	PDP	Proportion of discoverer population.
ADMM	Alternating direction multiplier method.	ISSA	Improved sparrow search algorithm.
LSTM	Long short-term memory.	SSA	Sparrow search algorithm.
SVM	Support vector machine.	GWO	Gray wolf optimization algorithm.
ELM	Extreme learning machine.	MFO	Moth fire optimization algorithm.
BPNN	Back propagation neural network.	PSO	Particle swarm optimization algorithm.
EMD	Empirical mode decomposition.	IMF	Intrinsic mode function.
EEMD	Ensemble empirical mode decomposition.	BIMF	Bandwidth intrinsic mode function.
CEEMD	Complementary Ensemble Empirical Mode Decomposition.	ISSA-VMD	Improved sparrow search algorithm-variational modal decomposition.
		ISSA-DBN	Improved sparrow search algorithm-deep belief network.
		OVMD-ODBN	Optimized variational modal decomposition-optimized deep belief neural network.

The associate editor coordinating the review of this manuscript and approving it for publication was Xiaodong Liang .

OVMD-DBN	Optimized variational modal decomposition-deep belief network.
OVMD-LSTM	Optimized variational modal decomposition-long short-term memory.
EMD-ODBN	Empirical mode decomposition-optimized deep belief neural network.
GBRBM	Gauss-Bernoulli-restricted Boltzmann machine.
RBM	Restricted Boltzmann machine.
RMSE	Root mean square error.
MAPE	Mean absolute percent error.
MAE	Mean absolute error.
R²	Coefficient of determination.
RBFNN	Radial basis function neural network.
ELMAN	Simple recurrent neural network

I. INTRODUCTION

Wind power output has strong random fluctuation and it is difficult to predict. The prediction deviation of wind power increases the rotary reserve cost required to maintain the stability of the power grid, and the excessive error may even lead to “off-grid” and other safety accidents. The power dispatching department often talks about wind change, which restricts the development of wind power to a certain extent [1], [2]. The accurate prediction of wind speed can effectively reduce the uncertain impact of wind power and improve the utilization of wind power in the power system. Therefore, it is necessary to predict the wind speed of wind farm.

At present, some scholars have carried out a lot of research on wind speed prediction, which is mainly divided into physical model method and intelligent prediction method. Physical model [3], [4] is mainly based on numerical weather forecast and topographic information, but it is vulnerable to the influence of the location of wind power plant and inherent physical characteristics of fans, and the adaptability of the method is poor. The intelligent method takes all kinds of external factors affecting load or historical load data as input and makes prediction based on various artificial intelligence methods, typical representatives of which are BP neural network and Support Vector Machine (SVM), etc. [5], [6], [7]. BP neural network [8] has many adjustable parameters and good operability, but its generalization ability is limited and it is easy to fall into local optimum. SVM can solve nonlinear and local minimum problems well, but the prediction accuracy is low when dealing with large-scale data. Deep learning algorithm is an extension of traditional artificial intelligence algorithm. Because it adopts multi-layer nonlinear transformation, it can more effectively represent the complex relationship in wind speed and wind power data. At present, it has become a research hotspot in new energy output prediction [9], [10]. Literature [11] proposed that the complete set empirical mode decomposition was used to preprocess data, and the combined model of long and short-term memory neural network and

BP network was used to build wind speed prediction model. Literature [12] proposed a combined model of convolutional neural network and bidirectional long and short-term memory neural network, in which convolutional neural network was used to propose the internal features of time series, and genetic algorithm was used to optimize the hyperparameters in the model. Literature [13] proposed a combination model combining wavelet transform and deep belief network, and made a comparative analysis with conventional prediction methods. Literature [14] proposed an adaptive deep learning model, which can realize automatic data learning and generate appropriate structure, and can capture the dynamic characteristics of wind speed data, thus achieving good wind speed prediction effect. However, the prediction methods in literature [11], [12], [13], and [14] are characterized by poor stability.

Due to the strong nonlinear characteristics of wind speed data, the single prediction method is rough, and it is difficult to refine the intrinsic law of the analysis data, and the prediction error is large. Wavelet decomposition, empirical mode function and other methods are used to decompose the data signal, and the prediction model of each component is established separately, which has gradually replaced the single prediction method. In literature [15] and [16], empirical mode decomposition method was used to decompose data series and further predict wind speed, but the modal aliasing problem existing in EMD could not be avoided. Literature [11] and [17] introduced improved EMD methods, including set empirical mode decomposition and complete set empirical mode decomposition, but the mode aliasing problem of EMD was not fundamentally solved. In literature [18] and [19], variational modal decomposition is used to decompose data sequence, which can effectively avoid the occurrence of modal aliasing. However, this method is not adaptive, and parameters such as decomposition number and penalty factor need to be determined.

In addition, some literatures discuss the use of swarm intelligence methods to optimize the parameters of prediction models, such as the optimization of VMD parameters and DBN parameters. These problems are essentially constrained programming mathematical problems, and the accuracy of the problem mainly depends on the optimization performance of intelligent algorithms, so the selection and optimization of solution methods is very important. Spark search algorithm [20] is a new intelligent optimization algorithm proposed in 2020. Compared with traditional intelligent optimization algorithms such as particle swarm optimization algorithm and gravitational search algorithm, this algorithm has advantages in search accuracy, convergence speed and stability. Scholar Li Yali [21] has made a detailed comparative study of the new swarm intelligent optimization algorithm that has emerged in recent years. It is concluded that the performance of sparrow search algorithm in convergence accuracy and stability is far better than that of bat algorithm, grey wolf optimization, whale optimization algorithm and other five optimization algorithms. However, as an algorithm

with excellent performance, SSA algorithm is rarely used by researchers to optimize the parameters of VMD and DBN, and few literatures consider optimizing the parameters of VMD and DBN at the same time.

Based on the above research, this paper introduces the improved sparrow algorithm and energy difference tracking method to adaptively optimize the key parameters of VMD, selects the depth belief network to establish the prediction model of each component, and uses the improved sparrow algorithm to optimize the super parameters of the prediction model. Finally, a combined wind speed prediction model of Issa to optimize VMD and DBN is proposed. The actual wind farm data in Northwest China are selected to verify the feasibility of this method. The main contributions of this study include the following:

- 1) An improved sparrow optimization algorithm based on reverse learning and cloud model theory is proposed to enhance the optimization ability of the algorithm.
- 2) The tracking method of energy difference is introduced, and an improved SSA algorithm is proposed to optimize the decomposition number and dependency factor of VMD.
- 3) An improved sparrow optimization algorithm is proposed and verified to optimize the structural parameters of DBN model.
- 4) The validity of the model is evaluated for the dates under different months.

The remainder of this article is organized as follows. Section 2 analyzes the improved sparrow intelligence algorithm and variational mode decomposition theory. Section 3 introduces deep belief networks and the implementation process of the ISSA-DBN prediction model. Section 4 carries on the experiment. The conclusions are drawn in Section 5.

II. VARIATIONAL MODAL DECOMPOSITION OPTIMIZED BY SPARROW ALGORITHM

A. VARIATIONAL MODAL DECOMPOSITION

VMD is a completely non-recursive mode variational method, which decomposes signal f into multiple mode functions u_k with certain sparse properties, and solves the problems of mode aliasing and high-frequency signal loss existing in EMD. The calculation formula of u_k bandwidth is shown in Formula (1) below:

$$\begin{cases} \min_{\{u_k\}, \{\omega_k\}} \sum_k \left\| \partial_t \left[\left(\delta(t) + \frac{j}{\pi t} \right) * u_k(t) \right] e^{-j\omega_k t} \right\|^2 \\ \text{s.t.} \sum_k u_k(t) = f(t) \end{cases} \quad (1)$$

In the formula, $\{u_k\}$ is the modal components and $\{\omega_k\}$ is the frequency center of each component.

Solve the above equation with the augmented Lagrange function, and obtain Equation (2):

$$\begin{aligned} L(\{u_k\}, \{\omega_k\}, \lambda) \\ = \alpha \sum_{k=1}^K \left\| \partial_t \left[\left(\delta(t) + \frac{j}{\pi t} \right) \cdot u_k(t) \right] e^{-j\omega_k t} \right\|^2 \end{aligned}$$

$$\begin{aligned} + \left\| f(t) - \sum_{k=1}^K u_k(t) \right\|^2 \\ + \left\langle \lambda(t), f(t) - \sum_{k=1}^K u_k(t) \right\rangle \end{aligned} \quad (2)$$

The formula above can be obtained by using the alternating direction multiplier method (ADMM):

$$\hat{u}_k^{n+1}(\omega) = \frac{\hat{f}(\omega) - \sum_{i \neq k} \hat{u}_i(\omega) + \hat{\lambda}(\omega)/2}{1 + 2\alpha(\omega - \omega_k)^2} \quad (3)$$

$$\omega_k^{n+1} = \frac{\int_0^\infty \omega |\hat{u}_k(\omega)| d\omega}{\int_0^\infty |\hat{u}_k(\omega)|^2 d\omega} \quad (4)$$

In the formula, $\hat{u}_k^{n+1}(\omega)$ and ω_k^{n+1} are wiener filtering and frequency center of each component respectively.

B. THE SPARROW ALGORITHM

Sparrow search algorithm (SSA) is a bionic intelligent algorithm proposed by Xue Jiankai *et al.* in 2020, which simulates the foraging and anti-predation behavior of sparrow population. When foraging, the whole sparrow population is divided into two fixed proportion of finders and entrants. According to the foraging rules, the finder guides the population search and foraging through location updating. Some participants chose to follow the finders to get food, while others chose to constantly monitor the finders and participate in food competition to increase their own predation rate. When the sparrow population is aware of the danger, the sparrows in different positions will choose the corresponding escape strategy. The above is a brief introduction of SSA algorithm, and the specific content can be found in literature [20] and [22].

The location of the finder is updated as follows:

$$x_{ij}^{t+1} = \begin{cases} x_{ij}^t \cdot \exp \left[\frac{-i}{\alpha \cdot \text{MaxCycle}} \right], & R_2 < \text{ST} \\ x_{ij}^t + QL \end{cases} \quad (5)$$

where, MaxCycle is the maximum number of iterations of the algorithm; α is uniform random number within interval (0, 1]; Q is a standard normal random number; L is the matrix of $1 \times d$ with an element value of 1; R_2 and ST are the set warning value and safety value respectively.

The location of the subscriber is updated as follows:

$$x_{ij}^{t+1} = \begin{cases} Q \cdot \exp \left[\frac{x_{wj}^t - x_{ij}^t}{i^2} \right], & i > NP/2 \\ x_{pj}^{t+1} + |x_{ij}^t - x_{pj}^t| A^+ L, & \text{其他} \end{cases} \quad (6)$$

where, x_{pj}^t is the optimal position of the discoverer in the t iteration; x_{wj}^t is the global worst position at the t iteration; NP is population number; A represents the matrix of $1 \times d$ whose elements are randomly assigned 1 or -1 , and $A^+ = A^T (AA^T)^{-1}$.

The location of the scouter is updated as follows:

$$x_{ij}^{t+1} = \begin{cases} x_{ij}^t + \beta |x_{ij}^t - x_{bj}^t|, & f_i \neq f_g \\ x_{ij}^t + K \frac{|x_{ij}^t - x_{wj}^t|}{f_i - f_w + \varepsilon}, & f_i = f_g \end{cases} \quad (7)$$

where, x_{bj}^t is the global optimal position in the t iteration; β is the step size control parameter, which follows normal distribution. K is a random number of $[-1, 1]$; f_i, f_g and f_w are the fitness value, global optimal value and global worst value of the current sparrow respectively.

C. IMPROVED SSA ALGORITHM

1) CHAOTIC SEQUENCE INITIALIZATION

SSA algorithm, like other intelligent algorithms, tends to fall into local optimum when solving complex optimization problems. In order to improve the global search ability of SSA algorithm, considering the randomness and ergodicity of chaos operator, the search range of the algorithm can be appropriately expanded to improve the solution accuracy of the algorithm. In view of the excellent performance of tent map in ergodic uniformity and convergence speed, this paper uses tent map to generate chaotic sequence for population initialization, and its mathematical model is as follows:

$$\begin{cases} x_{i+1} = x_i/\varphi, & 0 < x_i < \varphi \\ x_{i+1} = (1 - x_i)/(1 - \varphi), & \varphi < x_i < 1 \end{cases} \quad (8)$$

where, when $\varphi \in (0, 1)$ and $x \in [0, 1]$, the system (8) is in a chaotic state.

2) REVERSE LEARNING STRATEGY

In order to further improve the performance of the algorithm, a reverse learning strategy is introduced, through which the reverse solution of the optimal value can be obtained, and the search domain of the algorithm can be expanded, so that individuals can better find the optimal solution. Reverse learning was proposed by Tizhoosh in 2005. Based on the current solution, it seeks the corresponding reverse solution through reverse learning mechanism, and retains the superior solution as the next generation by comparing the original solution with the reverse solution. Suppose the individual sparrow is $x = (x_1, x_2 \dots, x_D)$, then the reverse point $x^* = (x_1^*, x_2^* \dots, x_D^*)$ corresponding to x is defined as:

$$x_j^* = a_j + b_j - x_j \quad (9)$$

In the formula, a_j and b_j are the upper and lower bounds of the value of the individual first dimension of sparrow respectively.

3) NORMAL CLOUD MODEL

Cloud model was proposed by the scholar Li Deyi in 1995 by integrating the theories of probability and statistics and fuzzy-theory [23]. It can realize the uncertain transformation between qualitative concepts and quantitative values, and the digital features of cloud are represented by expectation E_x ,

entropy E_n and hyper entropy H_e . The cloud model is characterized by stability in uncertainty and change in stability. The optimal solution of SSA algorithm can be taken as the center of the cloud model to search and compare the surrounding points, and then the optimal solution can be found. Normal cloud model is an important model in cloud theory, which can reflect the random probability distribution of nature and has great universality. Let C be a qualitative concept in the domain U of quantitative theory. If the quantitative value x is a random realization of the qualitative concept in the domain U and satisfies $x \sim N(E_x, En'^2)$, $En' \sim N(En, He^2)$, then the certainty of C can be expressed as:

$$\mu(x) = e^{-\frac{(x-E_x)^2}{2(En')^2}} \quad (10)$$

In the formula, $\mu(x)$ is a random number at $(0,1)$.

4) ISSA ALGORITHM

Combined with the previous sections, the steps of ISSA algorithm proposed in this paper can be summarized as follows:

Step 1: Initialize the algorithm parameters N , $Maxiter$, ST and the proportion of discoverer, joiner and scout in the sparrow population.

Step 2: The initial population is generated by using Equation (8).

Step 3: The population is updated by the sparrow algorithm, and the reverse population is generated by using Equation (9); And calculate the optimal individual.

Step 4: According to Section C, the position of the optimal solution is improved by using the normal cloud generator, and the optimal solution at this time is compared and determined.

Step 5: If $t < MaxCycle$, then $t = t + 1$, return to step 3, otherwise the algorithm ends.

D. OPTIMIZATION OF VMD BASED ON ISSA

When VMD is used for signal decomposition, parameters such as modal decomposition number, penalty factor, fidelity coefficient and convergence condition need to be preset. The study shows that the decomposition accuracy of VMD mainly depends on decomposition number K and penalty factor α . If the value of decomposition number K is set too small, information will be lost; if the value of decomposition number K is set too large, excessive decomposition will be caused. Penalty parameter α affects the bandwidth of each modal component, and different bandwidth scales affect the signal extraction results. Due to the complexity and variability of the actual signals to be decomposed, it is difficult to set the decomposition number K and penalty factor α artificially, and it is easy to lead to randomness of decomposition results [24]. Therefore, this paper proposes to optimize VMD parameters using ISSA algorithm.

The fitness function of ISSA's optimization of VMD parameters is based on the energy difference tracking method proposed in literature [25]. The basic idea is to decompose signal $f(t)$ into K finite Bandwidth Intrinsic Mode Function (BIMF) u_i according to VMD method, as shown in

TABLE 1. Benchmark functions.

Benchmark functions	dimensional	range	theoretical minimum
$f_1(x) = \sum_{i=1}^n x_i^2$	30	[-100,100]	0
$f_2(x) = \sum_{i=1}^n x_i + \prod_{i=1}^n x_i $	30	[-10,10]	0
$f_3(x) = \sum_{i=1}^n (\sum_{j=1}^i x_j)^2$	30	[-100,100]	0
$f_4(x) = \sum_{i=1}^n [x_i^2 - 10 \cos(2\pi x_i) + 10]$	30	[-5.12,5.12]	0
$f_5(x) = -20 \exp(-0.2 \sqrt{\frac{1}{n} \sum_{i=1}^n x_i^2}) - \exp(\frac{1}{n} \sum_{i=1}^n \cos(2\pi x_i)) + 20 + e$	30	[-32,32]	0
$f_6(x) = \frac{1}{4000} \sum_{i=1}^n x_i^2 - \prod_{i=1}^n \cos(\frac{x_i}{\sqrt{i}}) + 1$	30	[-600,600]	0

the following formula.

$$f(t) = u_1(t) + u_2(t) + \dots + u_k(t) = \sum_{i=1}^k u_i(t) \quad (11)$$

If BIMF satisfies orthogonality, then the energy of the original signal $f(t)$ (see Equation 12) is equal to the energy sum of K decomposed signals (see Equation 13).

$$E_{f1} = \int_{-\infty}^{+\infty} f^2(t) dt \quad (12)$$

$$E_{BIMF} = \int_{-\infty}^{+\infty} u_1(t) dt + \dots + \int_{-\infty}^{+\infty} u_k(t) dt \quad (13)$$

$$E_{f1} = E_{BIMF} \quad (14)$$

If the actual decomposition components of the signal are not all orthogonal, there is an energy error E_{err} between E_{f1} and E_{BIMF} .

$$E_{err} = |E_{f1} - E_{BIMF}| \quad (15)$$

The smaller E_{err} is, the better the orthogonality of decomposed BIMF component is, and the decomposition result can better characterize the characteristics of signal $f(t)$.

The solving steps of the optimal parameter combination $[K, \alpha]$ of VMD algorithm are as follows:

Step 1: Set the parameters of ISSA algorithm and the initial population, and take the energy error E_{err} as fitness function.

Step 2: VMD decomposition is performed on the signal, and the fitness value of each sparrow can be obtained by formula (15).

Step 3: According to the optimization mechanism of the sparrow algorithm, the individual positions of sparrows are updated, the corresponding energy error E_{err} of each position is compared, and the minimum fitness value is constantly updated.

Step 4: Cycle through step 2 ~ step 4 until the global minimum fitness value is determined or the maximum number of iterations is reached, and the optimal sparrow individual $[K, \alpha]$ is output.

Step 5: VMD decomposition of the signal is carried out by using the optimal parameter $[K, \alpha]$.

E. SIMULATION TEST OF ISSA AND OVMD

1) SIMULATION TEST OF ISSA

In order to verify the performance of SSA algorithm, it is compared and analyzed with common gray Wolf optimization algorithm (GWO), particle swarm optimization algorithm (PSO), and moth flame optimization algorithm (MFO). Different single-mode and multi-mode benchmark test function scenarios are selected, as shown in Table 1. Parameter Settings of each test algorithm are shown in Table 2. The number of population is set as 30, the number of iterations is set as 500, and the experimental results are the values of each method running independently for 30 times.

As can be seen from Table 3, ISSA and PSO, MFO and GWO algorithms have better optimization accuracy and stability in both single-mode and multi-mode test environments, and the single mode function optimization results of the improved ISSA algorithm are better than those of SSA algorithm. Except for f_5 , both of them have obtained theoretical values in multi-mode function optimization. From the time complexity, facing the complexity of the same problem, algorithm statement within the loop execution time mainly depends on the deepest level, as a result of the ISSA algorithm is introduced into chaos initialization, reverse learning optimization strategy as well as the method of normal cloud generation method into all did not increase the original scale, the cycle of SSA algorithm complexity so ISSA algorithm with SSA algorithm at the same time complexity, ISSA algorithm does not reduce the optimization timeliness of the original SSA algorithm. It can be seen intuitively from Figure 1 that ISSA algorithm has good convergence accuracy and fast convergence speed. According to the analysis results, ISSA has excellent performance in solving accuracy and adaptability.

TABLE 2. Algorithm parameter settings.

algorithm	Parameter Settings
SSA	ST = 0.6, PIP = 0.2, PDP = 0.7
ISSA	ST = 0.6, PIP = 0.2, PDP = 0.7
PSO	$w_{max} = 0.9, w_{min} = 0.2, c_1 = 0.2, c_2 = 0.2$
GWO	/
MFO	/

TABLE 3. Test results.

Test functions	Algorithm	optimal value	worst value	mean value	standard deviation
f_1	PSO	6.9325e-06	0.0010664	0.00025808	0.00032285
	GWO	7.3662e-29	9.2301e-27	2.1171e-27	3.9318e-27
	MFO	2.9179e-15	1.1083e-12	1.5971e-13	2.4164e-13
	SSA	0	3.1975e-44	1.0658e-45	5.8379e-45
	ISSA	0	0	0	0
f_2	PSO	0.0085095	0.11651	0.04128	0.044252
	GWO	1.668e-17	3.0099e-16	9.3935e-17	7.2904e-17
	MFO	1.7258e-10	10	0.66667	2.4944
	SSA	0	2.9308e-35	9.7944e-37	5.3505e-36
	ISSA	0	0	0	0
f_3	PSO	35.8112	234.7837	95.3043	40.1408
	GWO	5.9561e-09	6.917e-05	8.2136e-06	1.5219e-05
	MFO	0.00060796	5000.2023	333.4123	1247.2258
	SSA	0	1.4519e-55	4.9072e-57	2.6498e-56
	ISSA	0	0	0	0
f_4	PSO	26.168	90.662	53.9162	11.4587
	GWO	0	19.5007	3.3979	3.3209
	MFO	7.9597	58.7734	21.0007	11.2341
	SSA	0	0	0	0
	ISSA	0	0	0	0
f_5	PSO	0.001503	2.0224	0.23155	0.44577
	GWO	8.6153e-14	1.4655e-13	1.1043e-13	1.5047e-14
	MFO	1.2043e-08	18.2445	0.79687	3.5905
	SSA	8.8818e-16	8.8818e-16	8.8818e-16	0
	ISSA	8.8818e-16	8.8818e-16	8.8818e-16	0
f_6	PSO	1.0615e-06	0.027074	0.0068264	0.0072929
	GWO	0	0.036692	0.0039778	0.006954
	MFO	0.019678	0.36663	0.16852	0.12987
	SSA	0	0	0	0
	ISSA	0	0	0	0

2) SIMULATION TEST OF OVMD

To verify the effectiveness of OVMD decomposition signal, a test signal $y(t)$ is constructed, as shown in the following formula.

$$\begin{cases} y(t) = y_1(t) + y_2(t) + y_3(t) + y_4(t) \\ y_1(t) = \cos(100\pi t) \\ y_2(t) = 1.2 \cos(200\pi t) \\ y_3(t) = 1.5 \sin(300\pi t) \end{cases} \quad (16)$$

In the formula, y_4 is Gaussian noise with mean value of 0 and variance of 0.2. The sampling frequency f_s is 1kHz and the sampling point is 512.

ISSA population number is 20, iteration number is 30, the optimization range of K is set as [2, 14], the search range of α is set as [0, 2000], the parameter combination of VMD optimized by SSA algorithm is $[K, \alpha]$ as [4, 936], and the minimum energy error is 0.481. The OVMD decomposition results of $y(t)$ under this parameter are shown in Figure 2. The EMD method and OVMD method are compared and analyzed, and the EMD decomposition results are shown in Figure 3.

As can be seen from Figure 2, after OVMD decomposition of noisy signal $y(t)$, various frequency signals and noise signals can be separated, and the amplitude of component

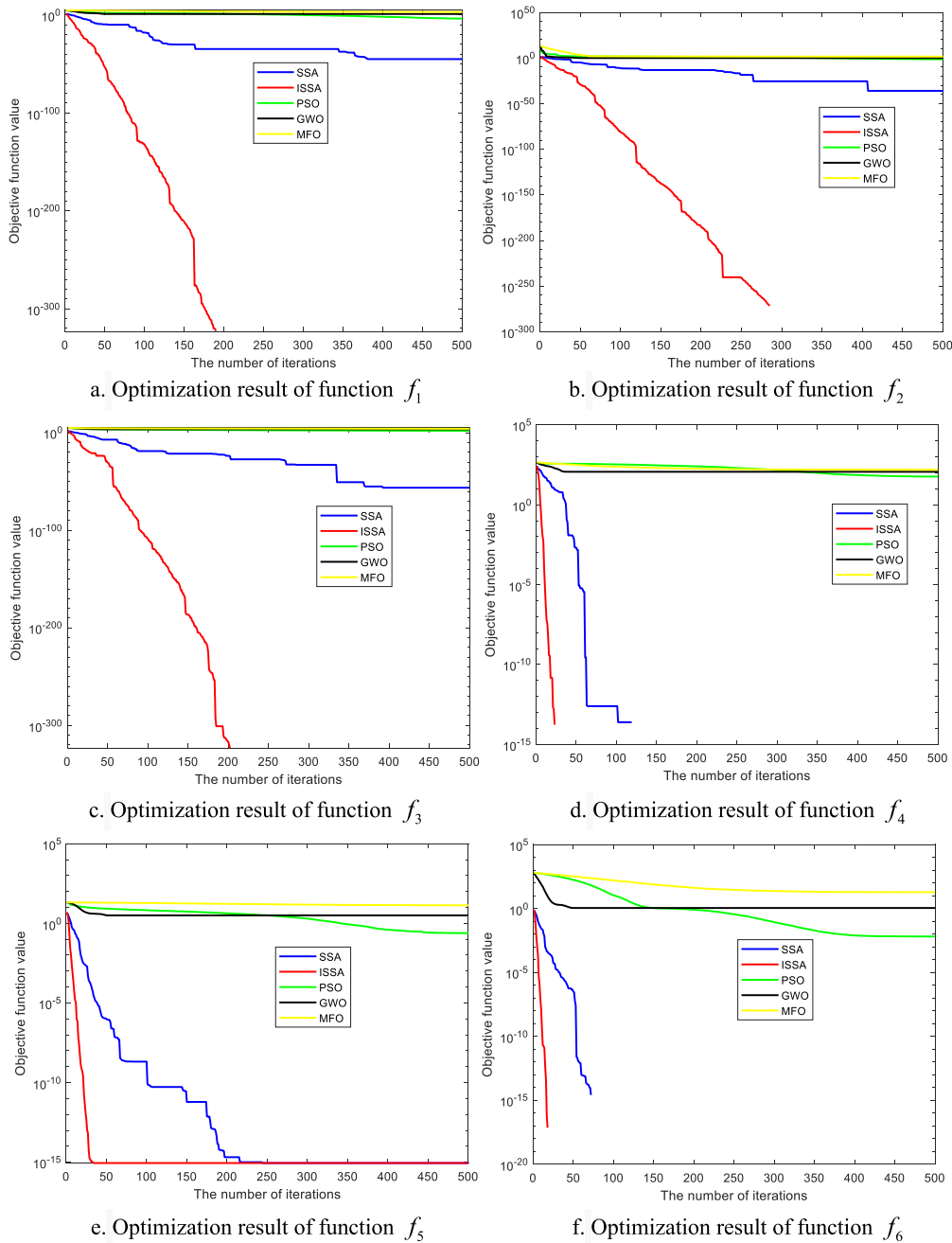


FIGURE 1. Fitness curve.

signals u_1 , u_2 and u_3 are also close to the original signal. As can be seen from Figure 4, there is obvious frequency aliasing in EMD decomposition components and the decomposition effect is poor. Therefore, OVMD method was used to decompose the wind speed series.

III. DBN NEURAL NETWORK AND OVMD-ODBN COMBINED PREDICTION MODEL

A. DEEP BELIEF NETWORK

Deep belief network (DBN) was proposed by Geoffrey Hinton [26], and its structure is shown in Figure 5. It is limited

by multiple restricted boltzmann machine (RBM) stack of feedforward neural networks, matter all connections between model layer, there is no connection in the layer, in which each matter including hidden layer h and visual v , the output of the previous matter layer as the next matter unit of input layer, the last of the whole network structure is controlled by a hidden layer and output layer structure of regression. Through input vector x and output vector y , the sample set $\{x, y\}$ of the prediction model is formed together.

RBM is a model based on the concept of energy, and the joint configuration energy function of the visible layer and

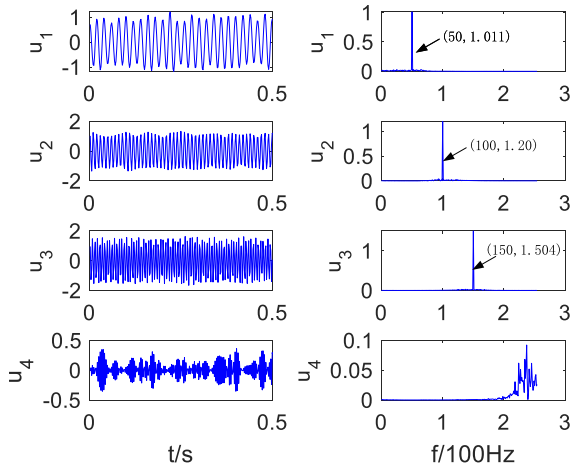


FIGURE 2. OVMD decomposition results.

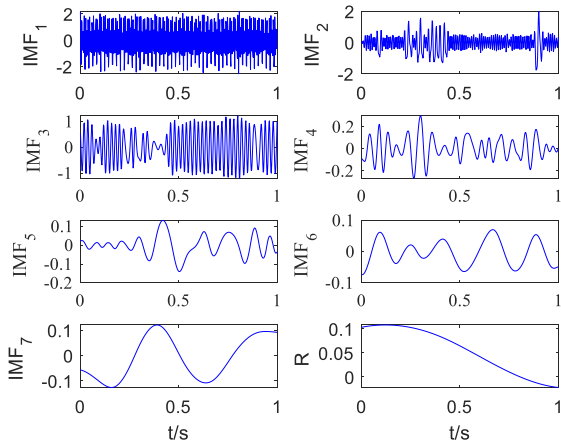


FIGURE 3. EMD decomposition results.

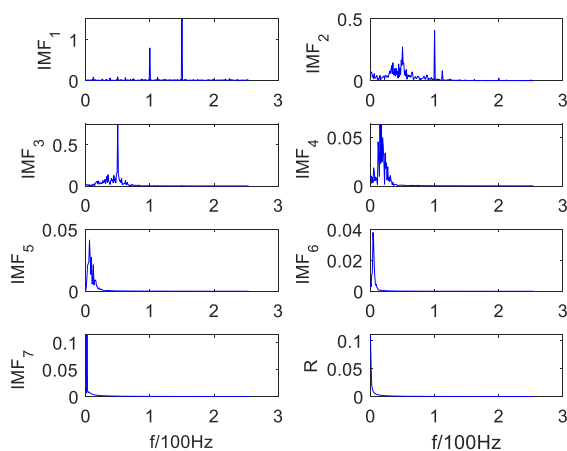


FIGURE 4. The spectrum of the decomposed components of EMD.

the hidden layer is

$$E(v, h | \theta) = - \sum_{ij} w_{ij} v_i h_j - \sum_i a_i v_i - \sum_j b_j h_j \quad (17)$$

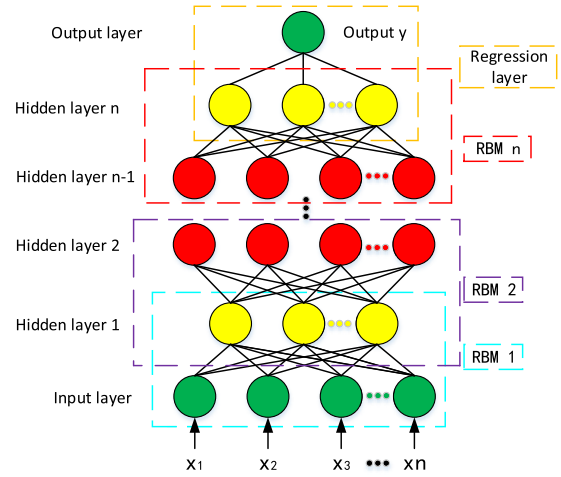


FIGURE 5. Structure of DBN.

In the formula, v_i and h_j represent the state of visible layer node and hidden layer node respectively. a_i and b_j represent the bias corresponding to visible layer node and hidden layer node respectively. w_{ij} represents the connection weight between the visible and hidden layers.

According to the above formula, the joint probability density of the visible layer and the hidden layer can be obtained

$$p(v, h | \theta) = \frac{1}{Z(\theta)} e^{-E(v, h | \theta)} \quad (18)$$

In the formula, $Z(\theta) = \sum_{v, h} e^{-E(v, h | \theta)}$ is the normalized factor.

In unsupervised learning, the purpose of training is to get parameters θ . For the training set containing N samples, the maximum likelihood function can be used

$$\theta^* = \arg \max_{\theta} L(\theta) = \arg \max_{\theta} \sum_{n=1}^N \log p(v^n | \theta) \quad (19)$$

DBN algorithm greedily pretrains RBM layer by layer, and then fine-tune and optimize the initial weight obtained by pre-training layer by layer using supervised back propagation algorithm, so that the model can obtain the optimal solution, and thus can characterize the complex nonlinear relationship in the wind speed data.

B. GAUSS-BERNOULLI CONSTRAINED BOLTZMANN MACHINE

For the standard deep belief network, the nodes of hidden layer and visible layer are Bernoulli values when sampling, while the input variables are continuous data when wind speed prediction. Therefore, gauss-Bernoulli Constrained Boltzmann machine (GBRBM) was introduced in this paper as the first RBM of DBN photovoltaic prediction model. Gaussian Bernoulli restricted Boltzmann machine introduces Gaussian function, so that the input vector is no longer limited to the Bernoulli distribution (binary distribution), which solves the problem of information loss when RBM processes

continuous input vectors. Firstly, continuous input data were converted into binary Bernoulli variables through GBRBM, and then further processed through standard RBM. This DBN is capable of processing continuous data and has functional modeling capabilities. The energy function of GBRBM is

$$E(v, h | \theta) = - \sum_{ij} \frac{v_i}{\sigma_i} w_{ij} h_j - \sum_i \frac{(v_i - a_i)^2}{2\sigma_i^2} - \sum_j b_j h_j \quad (20)$$

In the formula, v_i and h_j represent the states of visible layer nodes and hidden layer nodes respectively. At this point, v_i is a real-value input vector of wind speed sequence correlation factors, h_j value still conforms to Bernoulli type $\{0,1\}$ distribution, and σ is the standard deviation of Gaussian distribution. According to equations (21) and (22), the conditional probability of GBRBM visible layer and hidden layer units can be obtained.

$$p(v_i | h) = N(a_i + \sigma_i \sum_j w_{ij} h_j, \sigma_i^2) \quad (21)$$

$$p(h_j = 1 | v) = \text{sigmoid}(b_j + \sum_i \frac{v_i}{\sigma_i} w_{ij}) \quad (22)$$

In the formula, $N(\mu, \sigma_i)$ is a Gaussian function with mean value μ and standard deviation σ .

C. WIND SPEED PREDICTION MODEL BASED ON ISSA-DBN

Literature [27] points out that for specific sample data and DBN structure, setting appropriate parameters has an important impact on the modeling accuracy of DBN. The factors such as the number of hidden layers, the number of neurons in each layer and the learning rate in DBN are analyzed. It is concluded that the hidden layers of deep neural network should be set as 2 or 3 layers, and the model accuracy is high. When the number of hidden layers increases to 4, the classification or prediction effect of the model decreases and the generalization performance also decreases. In order to save the algorithm time, this paper selects the DBN network structure with 2 hidden layers, and uses the improved SSA optimization algorithm to optimize the number of neurons at 2 hidden layers and the learning rate of the whole DBN network.

For the two hidden layers of DBN, the number of neurons in each hidden layer is represented as m_1 and m_2 , and the learning rate is η . When coding the sparrow population in ISSA algorithm, each individual is a vector $X(m_1, m_2, \eta)$, then the optimization problem of DBN parameter can be expressed as:

$$F_{fitness}(m_1, m_2, \eta) = \frac{\sum_{i=1}^N (y_i - Y_i)^2}{N} \quad (23)$$

$$\text{s.t.} \begin{cases} 1 \leq m_1 \leq 100 \\ 1 \leq m_2 \leq 100 \\ 0 \leq \eta \leq 1 \end{cases} \quad (24)$$

In the formula, N is the number of samples, y_i and Y_i are the predicted value and true value of the first sample respectively.

See Figure 6 for the flow chart of ISSA optimization DBN, and the specific steps are as follows:

Step 1: Set the parameters of Issa algorithm and the initial population, code the individuals in the population, set each sparrow as a three-dimensional vector $X(m_1, m_2, \eta)$, select the population number as 20, set the maximum iteration number as 100, and set the threshold parameter ε as 0.001.

Step 2: The original wind speed data is decomposed by OVMD, and the generated component data is used as a test set, and the fitness value of each sparrow is obtained by formula (23).

Step 3: According to the sparrow algorithm optimization mechanism, the positions of individual sparrows are updated, the fitness function values corresponding to each position are compared, and the minimum fitness value is constantly updated.

Step 4: When the fitness function value is less than the threshold value ε or reaches the maximum number of iterations, the loop iteration ends, and the global minimum fitness value is determined to complete the optimization of DBN parameters.

D. OVMD-ODBN COMBINED PREDICTION MODEL

OVMD-ODBN proposed in this paper is shown in Figure 7, and the specific steps are as follows:

Step 1: Preprocess the wind speed data, query the singular values and missing data in the data, and fill them with cubic spline interpolation.

Step 2: OVMD decomposes the original wind speed sequence and obtains several training and test data sets of the DBN-network constructed by IMF.

Step 3: Initialize parameters such as the number of hidden layers and training times of DBN-network and the number of ISSA population and training times. ISSA algorithm is used to determine the number of neurons and the learning rate of each hidden layer in DBN network.

Step 4: Conduct pre-training and reverse fine-tuning on the determined DBN-network structure, and build DBN models corresponding to each IMF component.

Step 5: Start from the first moment of prediction, make multi-step rolling prediction, overlay and get the final wind speed value.

Step 6: Root mean square error (RMSE), mean absolute percentage error (MAPE), mean absolute error (MAE) and coefficient of determination (R^2) are selected to evaluate the performance of the prediction model.

$$\text{RMSE} = \sqrt{\frac{1}{N} \sum_{i=1}^N (s_i - s'_i)^2} \quad (25)$$

$$\text{MAPE} = \frac{1}{N} \sum_{i=1}^N \left| \frac{s_i - s'_i}{s_i} \right| \times 100\% \quad (26)$$

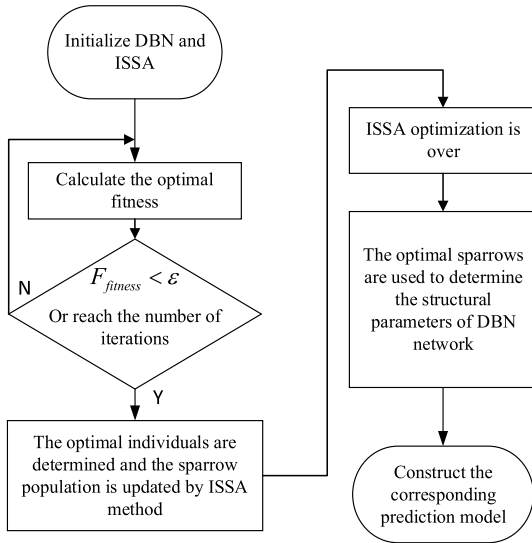


FIGURE 6. Flow chart of ISSA optimization DBN.

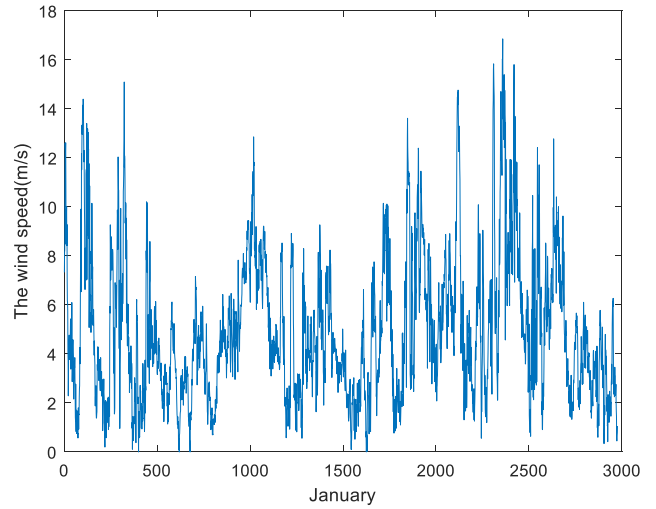


FIGURE 8. Original wind speed data.

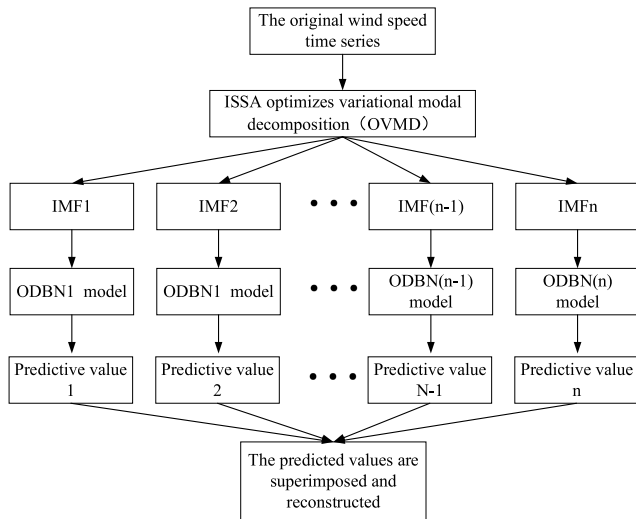


FIGURE 7. OVMD-ODBN combined prediction model.

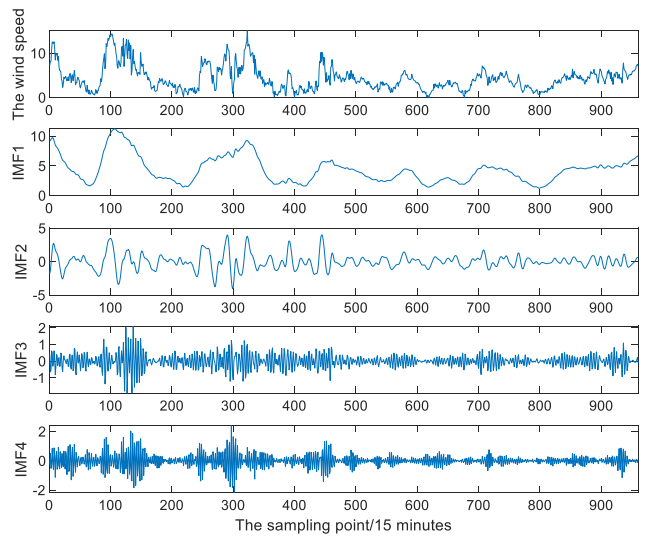


FIGURE 9. Decomposition results of OVMD.

$$MAE = \frac{1}{N} \sum_{i=1}^N |s_i - s'_i| \quad (27)$$

$$R^2 = 1 - \frac{\sum_{i=1}^N (s'_i - s_i)^2}{\sum_{i=1}^N (\bar{s}_i - s_i)^2} \quad (28)$$

In the formula, N is the number of samples; \bar{s}_i is the average of the true values; s_i and s'_i are the i true value and the predicted value respectively.

IV. EXPERIMENT AND RESULT ANALYSIS

A. ANALYSIS OF EXPERIMENTAL DATA

The wind speed data in January of a wind farm in northwest China is taken as the sample, and the resolution of wind speed

data is 15min. Taking the data from 2588-2976 in January as the sample population, the input and output data sets are set by using the method of predicting the data from the first five moments to the next moment. Among them, data from 2588-2880 are used as training data, and data from 2881-2776 are used as test samples. That is, 96 data are wind speed test data on January 31. See Figure 8 for wind power data. When the sample sequence is decomposed by the VMD method, the penalty parameter α and decomposition quantity value of VMD are optimized by the method described in section II, and the default values of other parameters are adopted. The decomposition results are shown in Figure 9.

As can be seen from Figure 9, the data quantity of IMF1 is the largest, but its frequency is low. The frequency of the other three columns increases gradually, but its value decreases gradually. In the prediction of wind speed data, the IMF1

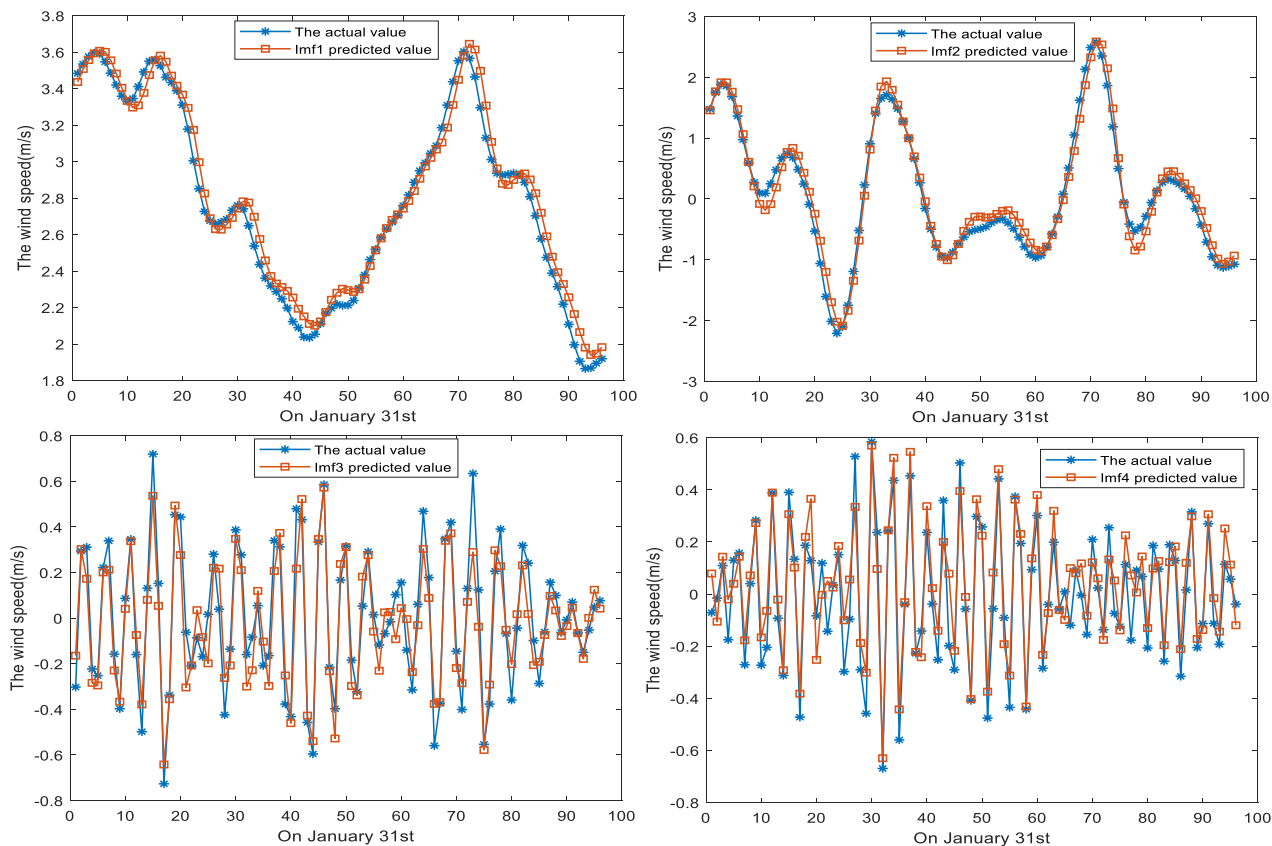


FIGURE 10. Prediction results of each component.

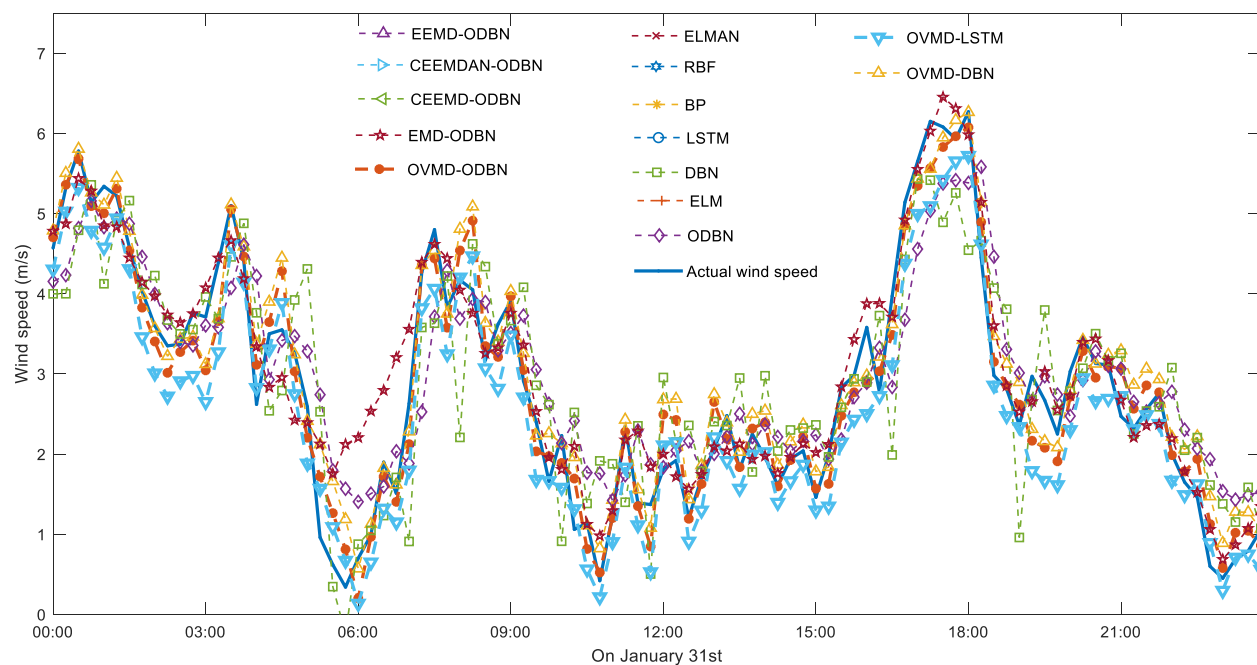


FIGURE 11. Prediction results of different prediction methods.

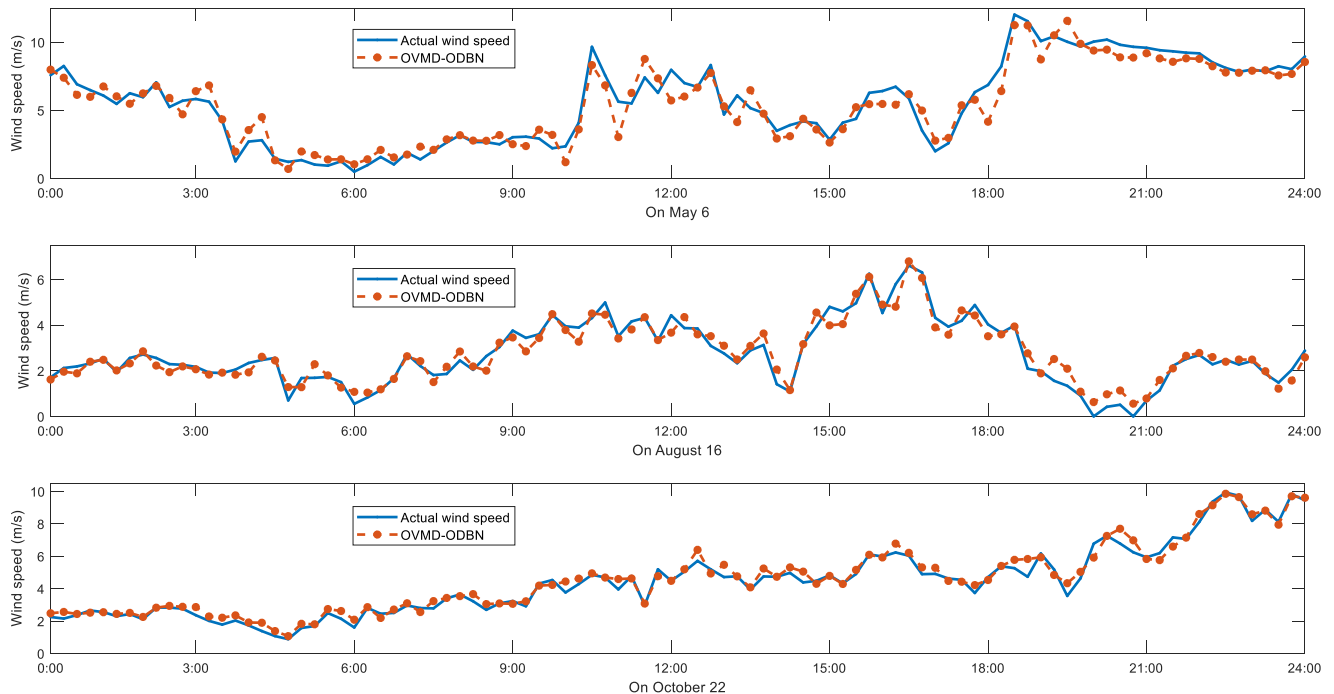


FIGURE 12. Prediction results of different forecast days.

component that plays a leading role in prediction accuracy is used.

B. ANALYSIS OF EXPERIMENTAL RESULTS

The comparison prediction models selected in this paper are shown in Table 4. The prediction method including ODBN, wherein the hidden layer value and learning rate of DBN are optimized according to part III of this paper. The conventional non-optimized DBN model is set with two RBM layers, the number of hidden layers is 50 and 100, the operation cycle is 300 generations, and the learning rate is 0.01. Parameter settings of other methods are as follows: The structural parameter of ELM is 102-35-1, the maximum iteration number is 500, and the activation function is *sig*. BP uses a single hidden layer, the structure parameters are 102-55-1, the learning rate is 0.01, and the maximum number of iterations is 500. The hidden layer of LSTM is set to 2, the time step is set to 20, and the learning rate is set to 0.05. The structural parameter of ELMAN is 15-35-1, the maximum iteration number is 500. The structural parameter of RBFNN is 19-30-1, the maximum iteration number is 500. In order to verify the performance of the proposed method in this paper, set up the comparison of four different scenarios, to make the results more convincing, considering the instability of neural network model to predict the results, the experimental results of the method are averaged, test times for 15 times, and the simulation results are shown in table 4, as shown in Figure 10 and 11, which obtained by OVMD four components, See Figure 9. Then, the corresponding ODBN model is

established to predict the four components, and the prediction results are shown in Figure 10. The final prediction results are obtained by superposing the values of each predicted component, as shown in Figure 11. As can be seen from Table 4, compared with LSTM and ELM and BP methods, RMSE index decreased by 0.0284m/s, 0.1723m/s and 0.2093m/s, MAPE index decreased by 1.193%, 4.2672% and 5.5939%, respectively. The results show that the prediction effect of DBN is better than that of LSTM, ELM and BP, among which the prediction effect of BP model is the worst, the prediction effect of LSTM model is better, but the prediction speed of LSTM method is the worst. ELM, LSTM and BP neural networks are not as stable as DBN. Compared with the ODBN method, the RMSE and MAPE indexes of the proposed OVMD-ODBN method decreased by 0.3731m/s and 8.7223%, respectively. Compared with the ODBN method, the RMSE and MAPE indexes of EMD-ODBN decreased by 0.2016m/s and 7.4064%, respectively. Compared with LSTM method, RMSE and MAPE indexes of OVMD-LSTM decreased by 0.3229m/s and 5.9793% respectively, indicating that the combined prediction model can accurately characterize the internal characteristics of each part of the signal due to the pretreatment and refinement operation of the prediction signal, and then carry out classification prediction. Therefore, the prediction effect is better than the single rough prediction method. It can be seen from Table 4 that compared with LSTM, ELM, BPNN, RBFNN and ELMAN methods, the RMSE index of DBN decreased by 0.0284m/s, 0.1723m/s, 0.2093m/s, 0.6879m/s and 0.0682m/s, and the MAPE index decreased by 1.193%, 4.2672%, 5.5939%,

TABLE 4. Error indicators of different prediction methods.

Prediction method	RMSE(m/s)	MAPE(%)	MAE	R ²
OVMD-ODBN	0.3621	7.6309	0.2879	0.9414
OVMD-DBN	0.4454	8.4502	0.3479	0.9113
ODBN	0.7352	16.3532	0.6030	0.7584
DBN	0.8115	17.9863	0.6512	0.7056
OVMD-LSTM	0.5170	13.2	0.4366	0.8805
EMD-ODBN	0.5336	8.9468	0.3838	0.8727
EEMD-ODBN	0.5849	11.0008	0.4822	0.8471
CEEMD-ODBN	0.6820	13.6636	0.6012	0.7921
CEEMDAN-ODBN	0.3945	7.6154	0.3278	0.9305
LSTM	0.8399	19.1793	0.6863	0.6847
ELM	0.9838	22.2535	0.7523	0.5674
BPNN	1.0208	23.5802	0.7758	0.5343
RBFNN	1.4994	27.0022	1.0641	-0.0049
ELMAN	0.8797	21.4284	0.7081	0.6541

TABLE 5. Error indicators of the method in this paper under different forecast days.

Forecast date	RMSE(m/s)	MAPE(%)	MAE	R ²
May 6	0.8702	10.1974	0.6911	0.9141
August 16	0.3814	9.0267	0.3049	0.9247
October 22	0.3637	5.1599	0.2784	0.9707

9.0159% and 3.4421% respectively. The results show that the prediction effect of DBN is better than other methods, among which RBFNN model has the worst prediction effect, LSTM and ELMAN model have better prediction results, but ELM, LSTM, BPNN and ELMAN are not as stable as DBN. Compared with OVMD-DBN, RMSE and MAPE indexes of OVMD-ODBN decreased by 0.0833m/s and 0.8193%, respectively, indicating that the DBN parameter optimization model proposed in this paper is better than the simple DBN parameter random setting method. It can be concluded from Table 4 and Table 5 that MAE and R² indexes of each method are consistent with RMSE and MAPE indexes, which verifies the rationality of the above analysis.

In order to further verify the generalization ability of the prediction method proposed in this paper, wind speed data in different months (May 6, August 16 and October 22) are selected as test objects to establish OVMD-ODBN model respectively. The final prediction curve is shown in Figure 12, and the error indicators are shown in Table 5. As can be seen from the chart, the predicted RMSE indexes for August 16 and October 22 are all less than 0.5m/s, and the distribution of MAPE indexes is less than 10%. The mean absolute error is also relatively small, R² index is close to 1. The overall prediction effect is good. Due to the large wind speed mutation on May 6, the prediction effect is not as good as the prediction effect of the previous two days, but the error is within 1m/s. Therefore, the prediction models proposed in this paper can meet the requirements of accurate prediction.

V. CONCLUSION

In order to improve the prediction accuracy of wind speed, OVMD-ODBN prediction model is proposed. Through experimental analysis, the following conclusions are drawn:(1) The prediction accuracy and stability of DBN method are better than that of LSTM, ELM and BP methods.(2) Optimization of decomposition number K and penalty factor α parameters of VMD method by ISSA algorithm can improve the signal adaptability of VMD method, and optimization of hidden layer unit number and learning rate of DBN prediction model by ISSA algorithm can optimize the performance of DBN prediction model. (3) The combined prediction model of OVMD-ODBN, OVMD-DBN and EMD-ODBN is better than the single DBN and ODBN method. From the whole prediction process, VMD variable IMF1 accounts for the largest proportion, but the prediction error is a little large, so the prediction accuracy of IMF1 component needs to be further improved. In addition, the empirical value and default value are used for VMD parameters in the experiment. In the next step, we will continue to study the comprehensive prediction effect of different methods according to different decomposition data characteristics.

REFERENCES

- [1] J. Hu and A. V. Vasilakos, "Energy big data analytics and security: Challenges and opportunities," *IEEE Trans. Smart Grid*, vol. 7, no. 5, pp. 2423–2436, Sep. 2016, doi: 10.1109/TSG.2016.2563461.

- [2] M. U. Yousuf, I. Al-Bahadly, and E. Avci, "Current perspective on the accuracy of deterministic wind speed and power forecasting," *IEEE Access*, vol. 7, pp. 159547–159564, 2019, doi: [10.1109/ACCESS.2019.2951153](https://doi.org/10.1109/ACCESS.2019.2951153).
- [3] C. Sasser, M. Yu, and R. Delgado, "Improvement of wind power prediction from meteorological characterization with machine learning models," *Renew. Energy*, vol. 183, pp. 491–501, Jan. 2022, doi: [10.1016/j.renene.2021.10.034](https://doi.org/10.1016/j.renene.2021.10.034).
- [4] H. Wang, N. Zhang, E. Du, J. Yan, S. Han, and Y. Liu, "A comprehensive review for wind, solar, and electrical load forecasting methods," *Global Energy Interconnection*, vol. 5, no. 1, pp. 9–30, Feb. 2022, doi: [10.1016/j.gloi.2022.04.002](https://doi.org/10.1016/j.gloi.2022.04.002).
- [5] Y. Wang, R. Zou, F. Liu, L. Zhang, and Q. Liu, "A review of wind speed and wind power forecasting with deep neural networks," *Appl. Energy*, vol. 304, Dec. 2021, Art. no. 117766, doi: [10.1016/j.apenergy.2021.117766](https://doi.org/10.1016/j.apenergy.2021.117766).
- [6] W. Sun, B. Tan, and Q. Wang, "Multi-step wind speed forecasting based on secondary decomposition algorithm and optimized back propagation neural network," *Appl. Soft Comput.*, vol. 113, Dec. 2021, Art. no. 107894, doi: [10.1016/j.asoc.2021.107894](https://doi.org/10.1016/j.asoc.2021.107894).
- [7] L. Xiang, Z. Deng, and A. Hu, "Forecasting short-term wind speed based on IEWT-LSSVM model optimized by bird swarm algorithm," *IEEE Access*, vol. 7, pp. 59333–59345, 2019, doi: [10.1109/ACCESS.2019.2914251](https://doi.org/10.1109/ACCESS.2019.2914251).
- [8] R. Li, Y. Dong, Z. Zhu, C. Li, and H. Yang, "A dynamic evaluation framework for ambient air pollution monitoring," *Appl. Math. Modell.*, vol. 65, Jan. 2019, pp. 52–71, doi: [10.1016/j.apm.2018.07.052](https://doi.org/10.1016/j.apm.2018.07.052).
- [9] M. Li, Z. Zhang, T. Ji, and Q. H. Wu, "Ultra-short term wind speed prediction using mathematical morphology decomposition and long short-term memory," *CSEE J. Power Energy Syst.*, vol. 6, no. 4, pp. 890–900, Dec. 2020, doi: [10.17775/CSEEJPES.2019.02070](https://doi.org/10.17775/CSEEJPES.2019.02070).
- [10] Z. Sun and M. Zhao, "Short-term wind power forecasting based on VMD decomposition, ConvLSTM networks and error analysis," *IEEE Access*, vol. 8, pp. 134422–134434, 2020, doi: [10.1109/ACCESS.2020.3011060](https://doi.org/10.1109/ACCESS.2020.3011060).
- [11] G. Chen, B. Tang, X. Zeng, P. Zhou, P. Kang, and H. Long, "Short-term wind speed forecasting based on long short-term memory and improved BP neural network," *Int. J. Electr. Power Energy Syst.*, vol. 134, Jan. 2022, Art. no. 107365, doi: [10.1016/j.ijepes.2021.107365](https://doi.org/10.1016/j.ijepes.2021.107365).
- [12] T. H. T. Nguyen and Q. B. Phan, "Hourly day ahead wind speed forecasting based on a hybrid model of EEMD, CNN-Bi-LSTM embedded with GA optimization," *Energy Rep.*, vol. 8, pp. 53–60, Nov. 2022, doi: [10.1016/j.egyr.2022.05.110](https://doi.org/10.1016/j.egyr.2022.05.110).
- [13] J. He, C. Yu, Y. Li, and H. Xi, "Ultra-short term wind prediction with wavelet transform, deep belief network and ensemble learning," *Energy Convers. Manage.*, vol. 205, Feb. 2020, Art. no. 112418, doi: [10.1016/j.enconman.2019.112418](https://doi.org/10.1016/j.enconman.2019.112418).
- [14] X. Mi and S. Zhao, "Wind speed prediction based on singular spectrum analysis and neural network structural learning," *Energy Convers. Manage.*, vol. 216, Jul. 2020, Art. no. 112956, doi: [10.1016/j.enconman.2020.112956](https://doi.org/10.1016/j.enconman.2020.112956).
- [15] Z. Jiang, J. Che, and L. Wang, "Ultra-short-term wind speed forecasting based on EMD-VAR model and spatial correlation," *Energy Convers. Manage.*, vol. 250, Dec. 2021, Art. no. 114919, doi: [10.1016/j.enconman.2021.114919](https://doi.org/10.1016/j.enconman.2021.114919).
- [16] L. Zhu and C. Lian, "Wind speed forecasting based on a hybrid EMD-BLS method," in *Proc. Chin. Automat. Congr. (CAC)*, Hangzhou, China, 2019, pp. 2191–2195.
- [17] B. K. Saxena, S. Mishra, and K. V. S. Rao, "Offshore wind speed forecasting at different heights by using ensemble empirical mode decomposition and deep learning models," *Appl. Ocean Res.*, vol. 117, Dec. 2021, Art. no. 102937, doi: [10.1016/j.apor.2021.102937](https://doi.org/10.1016/j.apor.2021.102937).
- [18] H. Hu, L. Wang, and R. Tao, "Wind speed forecasting based on variational mode decomposition and improved echo state network," *Renew. Energy*, vol. 164, pp. 729–751, Feb. 2021, doi: [10.1016/j.renene.2020.09.109](https://doi.org/10.1016/j.renene.2020.09.109).
- [19] F. He, J. Zhou, Z.-K. Feng, G. Liu, and Y. Yang, "A hybrid short-term load forecasting model based on variational mode decomposition and long short-term memory networks considering relevant factors with Bayesian optimization algorithm," *Appl. Energy*, vol. 237, pp. 103–116, Mar. 2019, doi: [10.1016/j.apenergy.2019.01.055](https://doi.org/10.1016/j.apenergy.2019.01.055).
- [20] J. Xue and B. Shen, "A novel swarm intelligence optimization approach: Sparrow search algorithm," *Syst. Sci. Control Eng.*, vol. 8, no. 1, pp. 22–34, Jan. 2020, doi: [10.1080/21642583.2019.1708830](https://doi.org/10.1080/21642583.2019.1708830).
- [21] Y. Li, S. Wang, Q. Chen, and X. Wang, "Comparative study of several new swarm intelligence optimization algorithms," *Comput. Eng. Appl.*, vol. 56, no. 22, pp. 1–12, 2020.
- [22] B. Li, H. Wang, X. Wang, M. Negnevitsky, and C. Li, "Tri-stage optimal scheduling for an islanded microgrid based on a quantum adaptive sparrow search algorithm," *Energy Convers. Manage.*, vol. 261, Jun. 2022, Art. no. 115639, doi: [10.1016/j.enconman.2022.115639](https://doi.org/10.1016/j.enconman.2022.115639).
- [23] W. Song and J. Zhu, "A goal-reference-point decision-making method based on normal cloud model and its application in distribution network planning evaluation," *Inf. Sci.*, vol. 577, pp. 883–898, Oct. 2021, doi: [10.1016/j.ins.2021.08.064](https://doi.org/10.1016/j.ins.2021.08.064).
- [24] J. Gai, J. Shen, Y. Hu, and H. Wang, "An integrated method based on hybrid grey wolf optimizer improved variational mode decomposition and deep neural network for fault diagnosis of rolling bearing," *Measurement*, vol. 162, Oct. 2020, Art. no. 107901, doi: [10.1016/j.measurement.2020.107901](https://doi.org/10.1016/j.measurement.2020.107901).
- [25] C. Junsheng, Y. Dejie, and Y. Yu, "Research on the intrinsic mode function (IMF) criterion in EMD method," *Mech. Syst. Signal Process.*, vol. 20, no. 4, pp. 817–824, May 2006, doi: [10.1016/j.ymsp.2005.09.011](https://doi.org/10.1016/j.ymsp.2005.09.011).
- [26] G. E. Hinton, S. Osindero, and Y.-W. Teh, "A fast learning algorithm for deep belief nets," *Neural Comput.*, vol. 18, no. 7, pp. 1527–1554, 2006, doi: [10.1162/neco.2006.18.7.1527](https://doi.org/10.1162/neco.2006.18.7.1527).
- [27] Y. Li, L. Wang, and L. Jiang, "Rolling bearing fault diagnosis based on DBN algorithm improved with PSO," *J. Vib. Shock*, vol. 39, pp. 89–96, May 2020.



LIJUAN ZHU received the M.Sc. degree from the Kunming University of Science and Technology, in 2016. She is currently a Lecturer with the Xinjiang Institute of Technology. Her research interests include artificial intelligence and image processing.



WEI HU received the M.Sc. degree from the Kunming University of Science and Technology, in 2016. He is currently pursuing the Ph.D. degree with Xinjiang University. His current research interests include renewable energy forecasting and capacity configuration of energy storage systems.